

# Crystal Structures of Cytochrome P-450<sub>CAM</sub> Complexed with Camphane, Thiocamphor, and Adamantane: Factors Controlling P-450 Substrate Hydroxylation<sup>†,‡</sup>

Reetta Raag<sup>§</sup> and Thomas L. Poulos\*

Center for Advanced Research in Biotechnology of the Maryland Biotechnology Institute, University of Maryland at Shady Grove, 9600 Gudelsky Drive, Rockville, Maryland 20850, and the Department of Chemistry and Biochemistry, University of Maryland, College Park, Maryland 20742-5115

Received September 26, 1990; Revised Manuscript Received December 4, 1990

**ABSTRACT:** X-ray crystal structures have been determined for complexes of cytochrome P-450<sub>CAM</sub> with the substrates camphane, adamantane, and thiocamphor. Unlike the natural substrate camphor, which hydrogen bonds to Tyr96 and is metabolized to a single product, camphane, adamantane and thiocamphor do not hydrogen bond to the enzyme and all are hydroxylated at multiple positions. Evidently the lack of a substrate-enzyme hydrogen bond allows substrates greater mobility in the active site, explaining this lower regiospecificity of metabolism as well as the inability of these substrates to displace the distal ligand to the heme iron. Tyr96 is a ligand, via its carbonyl oxygen atom, to a cation that is thought to stabilize the camphor-P-450<sub>CAM</sub> complex [Poulos, T. L., Finzel, B. C., & Howard, A. J. (1987) *J. Mol. Biol.* 195, 687-700]. The occupancy and temperature factor of the cationic site are lower and higher, respectively, in the presence of the non-hydrogen-bonding substrates investigated here than in the presence of camphor, underscoring the relationship between cation and substrate binding. Thiocamphor gave the most unexpected orientation in the active site of any of the substrates we have investigated to date. The orientation of thiocamphor is quite different from that of camphor. That is, carbons 5 and 6, at which thiocamphor is primarily hydroxylated [Atkins, W. M., & Sligar, S. G. (1988) *J. Biol. Chem.* 263, 18842-18849], are positioned near Tyr96 rather than near the heme iron. Therefore, the crystallographically observed thiocamphor-P-450<sub>CAM</sub> structure may correspond to a nonproductive complex. Disordered solvent has been identified in the active site in the presence of uncoupling substrates that channel reducing equivalents away from substrate hydroxylation toward hydrogen peroxide and/or "excess" water production. A buried solvent molecule has also been identified, which may promote uncoupling by moving from an internal location to the active site in the presence of highly mobile substrates.

The cytochrome P-450 superfamily of enzymes catalyzes many different types of oxidative reactions involved in steroid hormone biosynthesis, fatty acid metabolism, and detoxification of foreign compounds (Nebert et al., 1981; Nebert & Gonzalez, 1987; Anders, 1985). Xenobiotic-metabolizing P-450s generally oxidize substrates to more soluble forms, facilitating their excretion. Occasionally these products linger in the cytoplasm as "activated" electrophilic compounds, many of which are mutagens and/or carcinogens (Heidelberger, 1975; Sato & Omura, 1978; Anders, 1985; Ortiz de Montellano, 1986; Wolf, 1986). Due to the broad substrate specificity of this superfamily, and its ability to catalyze multiple types of reactions, there is much interest in structure-function relationships of P-450s. Ultimate goals include designing compounds to selectively inhibit individual P-450s and engineering novel P-450s to facilitate detoxification of specific environmental contaminants.

The best characterized P-450, and the only one for which a crystal structure is known, is the bacterial camphor hydroxylase P-450<sub>CAM</sub> (Gunsalus et al., 1974; Debrunner et al.,

1978; Gunsalus & Sligar, 1978; Ullrich, 1979; Wagner & Gunsalus, 1982; Poulos et al., 1985, 1987). The reaction cycle of cytochrome P-450<sub>CAM</sub> is shown in Figure 1. Besides hydroxylating camphor, P-450<sub>CAM</sub> will also hydroxylate various other compounds. We have determined the X-ray crystal structures of ferric cytochrome P-450<sub>CAM</sub> complexed with different substrates and inhibitors, as well as in the ferrous carbon monoxide and camphor bound form (Raag & Poulos, 1989a,b, 1990; Raag et al., 1990). These structures, together with data on substrate-dependent parameters and site-directed mutagenesis of P-450s (White et al., 1984; Fisher & Sligar, 1985; Atkins & Sligar, 1988a,b), have enabled us to better understand factors that influence regiospecificity and efficiency of P-450 reactions. Here we extend these studies to include three additional substrates. All substrate-P-450<sub>CAM</sub> coordinates have been submitted to the Brookhaven Protein Data Bank (Bernstein et al., 1977).

## MATERIALS AND METHODS

Thiocamphor synthesis was according to Scheeren et al. (1973) with the exception that P<sub>2</sub>S<sub>5</sub> (FLUKA, Ronkonkoma, NY) was used in place of P<sub>4</sub>S<sub>10</sub>. Samples were analyzed (Galbraith Laboratories, Knoxville, TN) for C, H, O, and S to confirm that the correct compound had been prepared. P-450<sub>CAM</sub> was crystallized according to our earlier procedure (Poulos et al., 1982). To prepare the various substrate-P-450<sub>CAM</sub> complexes, crystals were soaked in a mother liquor

<sup>†</sup> Supported in part by NIH Grant GM 33688.

<sup>‡</sup> Crystallographic coordinates have been submitted to the Brookhaven Protein Data Bank under the following file names: 4CPP, cytochrome P-450<sub>CAM</sub>-adamantane; 6CPP, cytochrome P-450<sub>CAM</sub>-camphane; 8CPP, cytochrome P-450<sub>CAM</sub>-thiocamphor.

\* Correspondence should be addressed to T.L.P. at CARB.

<sup>§</sup> University of Maryland.

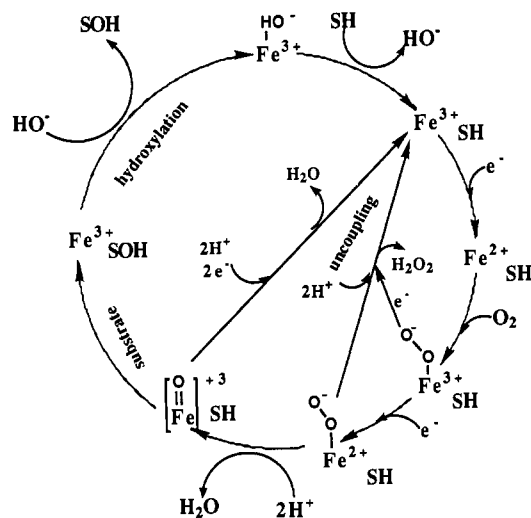


FIGURE 1: P-450 reaction cycle [modified from Atkins and Sligar (1988a)]. SH and SOH represent substrate and oxidized substrate, respectively. "Uncoupling" reactions compete with substrate hydroxylation. "Efficiency" refers to the percentage of reducing equivalents utilized toward substrate oxidation, as opposed to hydrogen peroxide/"excess" water production.

Table I: Summary of Substrate-P-450 Data Collection

substrate	camphane	adamantane	thiocamphor
max resolutn	1.91 Å	2.11 Å	2.09 Å
total observatns	108 560	144 737	133 336
$R_{\text{sym}}^a$	0.067	0.079	0.058
% data collected to	3.47 Å, 100%	3.82 Å, 100%	3.79 Å, 100%
	2.76 Å, 100%	3.04 Å, 100%	3.01 Å, 100%
	2.41 Å, 100%	2.65 Å, 100%	2.63 Å, 100%
	2.19 Å, 100%	2.41 Å, 100%	2.39 Å, 100%
	2.03 Å, 72%	2.24 Å, 100%	2.22 Å, 100%
	1.91 Å, 45%	2.11 Å, 73%	2.09 Å, 54%
$I/\sigma(I)$	2.19 Å, 1.91	2.41 Å, 2.50	2.13 Å, 2.15
	2.03 Å, 1.08	2.24 Å, 1.46	2.11 Å, 2.13
	1.91 Å, 0.55	2.11 Å, 0.72	2.09 Å, 0.24

<sup>a</sup>  $R_{\text{sym}} = \sum |I_i - \langle I_i \rangle| / \sum I_i$  where  $I_i$  = intensity of the  $i$ th observation and  $\langle I_i \rangle$  = mean intensity.

consisting of 40% saturated ammonium sulfate, 0.05 M potassium phosphate, and 0.25 M KCl at pH 7.0, with saturating amounts of camphane, adamantane, or thiocamphor. Soak times were about three to four days. X-ray diffraction data were collected from single crystals of the various substrate-P-450<sub>CAM</sub> complexes by using a Siemens area detector/Rigaku rotating anode and processed by using the XENGEN program package (Howard et al., 1987) on a Digital Equipment Corporation Microvax II. Data collection statistics are presented in Table I.

Substrates were initially sketched by using the Chemnote two-dimensional molecular construction facility in the molecular modeling package QUANTA (Polygen Corp., Waltham, MA), installed on a Silicon Graphics IRIS workstation. Following two-dimensional model building, substrate coordinates were energy minimized, again through QUANTA, using CHARMM steepest descents and Newton-Raphson energy minimization procedures. Substrate van der Waals volumes were calculated with QUANTA as well. Thiocamphor was modeled by substituting sulfur for oxygen in camphor, with the sulfur-carbon bond length maintained at the corresponding value for the oxygen-carbon bond. Such a model for thiocamphor should be adequate since the bond orders of C=S and C=O bonds are similar (Demarco et al., 1969).

Crystallographic refinement was carried out by using the restrained parameters-least squares package of programs

Table II: Summary of Substrate-P-450 Crystallographic Refinement

substrate	camphane	adamantane	thiocamphor
resolutn range (Å)	10.0–1.9	10.0–2.1	10.0–2.1
reflectns measured	27 786	20 548	22 650
reflectns used <sup>a</sup>	20 585	15 174	19 565
$R$ factor <sup>b</sup>	0.190	0.184	0.175
rms deviation of bond dist (Å)	0.020	0.019	0.020
bond angles (Å)	0.032	0.033	0.033
dihedral angles (Å)	0.036	0.037	0.036

<sup>a</sup> Reflections with  $I > 2\sigma(I)$ ;  $I$  = intensity. <sup>b</sup>  $R = \sum |F_o - F_c| / \sum F_o$ .

(Hendrickson & Konner, 1980) and is summarized in Table II. Initial  $F_o - F_c$  and  $2F_o - F_c$  difference Fourier maps were based on structure factor calculations using coordinates from the 1.7-Å refined camphor-P-450<sub>CAM</sub> structure (Poulos et al., 1987) and diffraction data obtained from the substrate-P-450<sub>CAM</sub> complexes. Camphor coordinates were not included in the initial structure factor calculations.  $F_o - F_c$  maps were contoured at  $\pm 3\sigma$  and  $2F_o - F_c$  maps were contoured at  $+0.5$  and  $+1\sigma$  ( $\sigma$  is the standard deviation calculated over an entire asymmetric unit of the electron density map). Substrates were positioned into the  $F_o - F_c$  maps and refined together with the protein, with substrate temperature factors initially starting at 19–20 Å<sup>2</sup>, or near the mean temperature factor for all protein and heme atoms in the camphor-P-450<sub>CAM</sub> structure. Structures were judged to have refined sufficiently once  $F_o - F_c$  maps showed little or no interpretable density when contoured at  $3\sigma$ . Initial  $F_o - F_c$  and final  $2F_o - F_c$  maps are shown in Figures 2 and 3. Refined models were subjected to additional refinement without bond, angle, or nonbonded contact distance restraints to better estimate active site distances. Comparison of both coordinate and temperature factor shifts was carried out as described elsewhere (Poulos & Howard, 1987).

## RESULTS

Figures 2 and 3 show the initial  $F_o - F_c$  and final  $2F_o - F_c$  maps of the camphane-, adamantane-, and thiocamphor-P-450<sub>CAM</sub> complexes. Modeling of camphane and adamantane bound to the enzyme was relatively straightforward. However, neither adamantane nor camphane is able to hydrogen bond to P-450<sub>CAM</sub> and so we cannot be sure that these substrates do not occupy multiple orientations. Since models with single orientations for these substrates were successful in eliminating most of the difference electron density from the active site region, we take this as evidence that at least the *major* binding orientations of these substrates have been identified.

**Camphane.** Despite the similarity in structure and binding orientation between camphane and camphor, the atomic temperature factors of camphane refined to values (30 Å<sup>2</sup>) about twice those of camphor (16 Å<sup>2</sup>). This indicates that camphane is highly mobile when bound to P-450<sub>CAM</sub>. One factor that could artificially raise temperature factors is an inaccurate model. We modeled the observed active site electron density with a single, fully occupied camphane molecule, but such a model would be inaccurate if the camphane occupancy in the crystal was incomplete. This is feasible since neither camphane nor adamantane was especially soluble in the crystallization mother liquor. However, since we were able to successfully model these substrates with full occupancy, the contribution

<sup>1</sup> Abbreviations:  $F_c$ , calculated structure factors;  $F_o$ , observed structure factors; L6, sixth or distal ligand to heme iron;  $R$  factor,  $\sum |F_o - F_c| / \sum F_o$ .

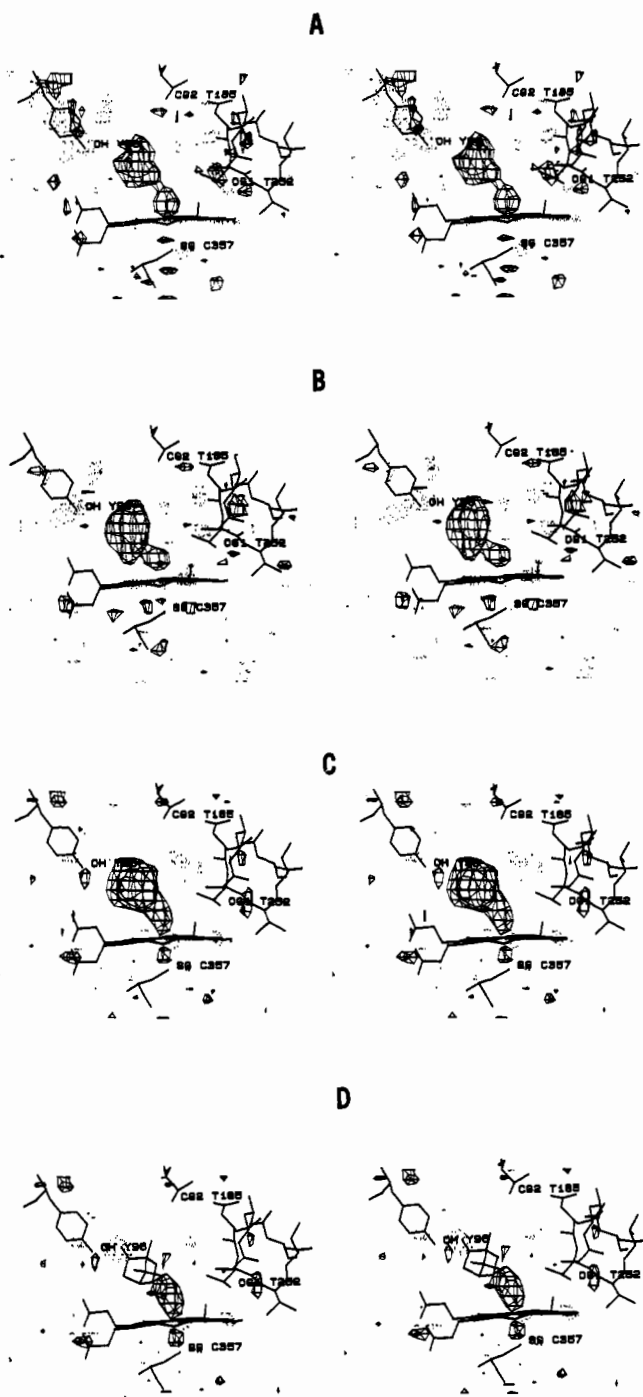


FIGURE 2: Initial  $F_o - F_c$  difference electron density maps for P-450<sub>CAM</sub> complexed with camphane (A), adamantane (B), and thiocamphor (C, D). Maps were calculated with diffraction amplitudes from substrate-P-450<sub>CAM</sub> complexes and phases from camphor-P-450<sub>CAM</sub> coordinates (Poulos et al., 1987). Maps are contoured at  $\pm 3\sigma$  with negative and positive density depicted as dotted and solid lines, respectively. Substrate coordinates were not included in phase calculations for maps A, B, and C, but camphor coordinates were included in the calculation of map D. Map D, with the camphor carbonyl oxygen in negative density and with positive density between the substrate and heme, indicates that thiocamphor binds "upside down" in the active site, compared with camphor. Note the electron density corresponding to the distal ligand to iron in all maps.

from the substrate-free structure is probably minimal (less than 20%). The presence of minor, unmodeled, binding orientations due to the lack of an enzyme-substrate hydrogen bond also could artificially raise substrate temperature factors.

With these caveats in mind, we still believe the high temperature factor of camphane is genuine. One reason is that

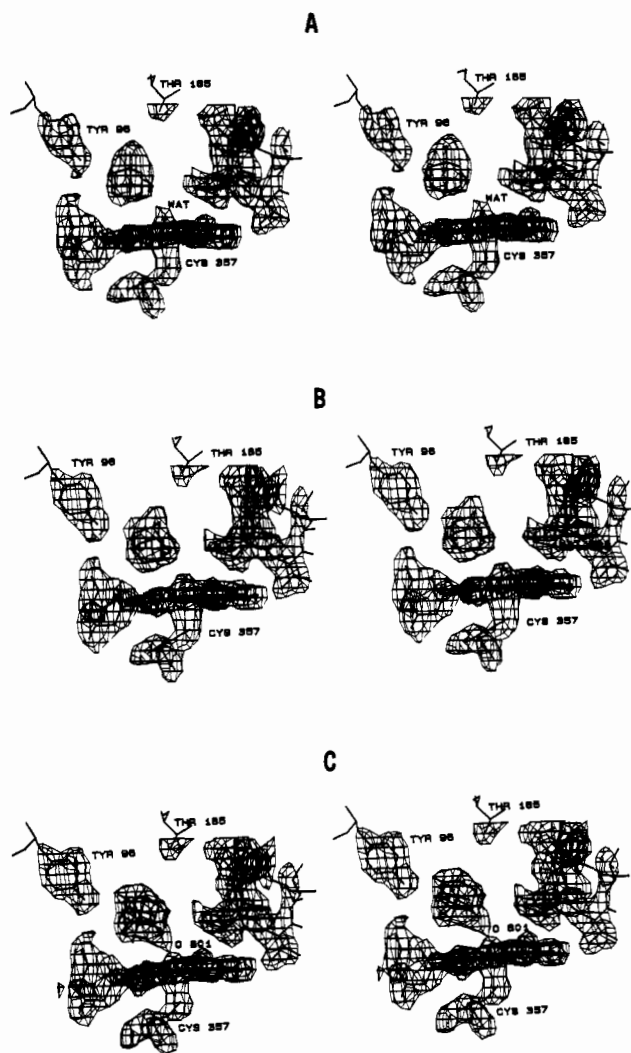


FIGURE 3: Final  $2F_o - F_c$  electron density maps for P-450<sub>CAM</sub> complexed with camphane (A), adamantane (B), and thiocamphor (C). Substrate and distal ligand coordinates were omitted from phase calculations for the maps shown. Note the electron density corresponding to the distal ligand to iron in all maps.

the temperature factors of Tyr96 side-chain atoms in the camphane-P-450<sub>CAM</sub> structure are in the vicinity of  $28 \text{ \AA}^2$  and only about  $13 \text{ \AA}^2$  in the camphor-P-450<sub>CAM</sub> complex, suggesting that the high camphane atomic temperature factors are real.

**Adamantane.** Temperature factors of Tyr96 side-chain atoms were about  $19 \text{ \AA}^2$  in adamantane-bound and  $10 \text{ \AA}^2$  in adamantane-bound P-450<sub>CAM</sub> structures. These values are consistent with the lower average temperature factor of adamantane ( $24 \text{ \AA}^2$ ) than camphane and indicate that adamantane is less mobile than camphane when bound by P-450<sub>CAM</sub>. We were concerned about this implication, considering that adamantane is highly symmetric and smaller than camphane and that neither substrate is able to hydrogen bond to the enzyme. Therefore we performed several refinement experiments.

Using the refined coordinates for adamantane-P-450<sub>CAM</sub>, with an  $R$  factor of 18.1%, we repositioned adamantane in the substrate electron density in two different ways: (1) by approximately switching the locations of secondary and tertiary carbons and (2) by approximately switching the locations of atoms and bonds. Both of these repositionings resulted in a somewhat poorer fit of the substrate to the electron density. Next, 10 cycles of refinement were conducted in which tem-

perature factors of all atoms and occupancies of solvent atoms were refined alternately. In both experiments, the average temperature factor of adamantane increased by about 2.5 Å<sup>2</sup> (to 26.1 and 25.9 Å<sup>2</sup>, respectively). Ten control refinement cycles increased the temperature factor of the best-fit adamantane model by approximately 1.0 Å<sup>2</sup> to 24.7 Å<sup>2</sup>. In all three cases, the *R* factor dropped only 0.1% to 18.0%. However, electron density maps calculated with both sets of repositioned coordinates contained substantial amounts of  $\pm 3\sigma$   $F_o - F_c$  difference electron density, indicating that the substrate was incorrectly positioned.

Our next two experiments involved fixing the temperature factors of all adamantane atoms arbitrarily at 16.0 and 32.0 Å<sup>2</sup> and calculating electron density maps to determine if there would be any observable effects. No differences were found either in *R* factor or in electron density maps when refined adamantane temperature factors (23.6 Å<sup>2</sup> average) or arbitrary ones of 32.0 Å<sup>2</sup> were used. However, when adamantane atomic temperature factors were set to 16.0 Å<sup>2</sup>, although the *R* factor remained at 18.0%, positive 3 $\sigma$  difference electron density appeared around the substrate in the  $F_o - F_c$  map, suggesting that the new temperature factors were incorrect.

In the final adamantane refinement experiment, the adamantane model considered best fit to the electron density was again used but all substrate atomic temperature factors were started at 32.0 Å<sup>2</sup>. After 10 refinement cycles, the average atomic temperature factor for adamantane rose insignificantly to 32.1 Å<sup>2</sup>, rather than dropping toward the previously determined value of 23.6 Å<sup>2</sup>. Once again, the *R* factor remained at 18.0% and difference electron density maps showed no indication that substrate temperature factors might be incorrect. On the basis of these refinement experiments, we cannot give a definitive value for the adamantane temperature factor, but we regard it as being somewhere in the neighborhood of 25–32 Å<sup>2</sup>.

**Thiocamphor.** In the initial thiocamphor  $F_o - F_c$  map, which was based on camphor-P-450<sub>CAM</sub> coordinates without camphor included, the substrate appeared to be binding "upside down" with respect to camphor (Figure 2C). Thus a second  $F_o - F_c$  map was calculated, again based on the camphor-P-450<sub>CAM</sub> coordinates, but this time including camphor coordinates, in their original orientation, in the phase calculation. When this map was contoured at  $\pm 3\sigma$ , the camphor carbonyl oxygen was found to occupy a region of negative difference electron density and a large region of positive difference electron density remained between the substrate and heme (Figure 2D). Although it seemed apparent that thiocamphor and camphor do not bind to P-450<sub>CAM</sub> in the same orientation, another map was calculated, based on coordinates in which thiocamphor occupied the same orientation as camphor and in which an additional water molecule was included to occupy the positive density near the distal heme ligation site. As expected, the thiocamphor sulfur atom was surrounded by negative density and the water ligand was insufficient to account fully for the positive density between thiocamphor and the heme. Next, the distal water ligand was removed and thiocamphor was rotated (by approximately 180° in the plane of Figures 2 and 3) so that the thiocarbonyl was no longer directed toward Tyr96 but was directed toward the heme iron. Maps based on this model contained much less difference electron density but some positive difference density still remained between the sulfur and the heme iron. After including the distal ligand again, with thiocamphor in the new "upside down" orientation (Figure 4A), only a small amount of positive and negative difference density remained to either side of the

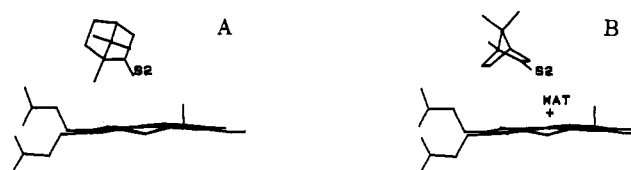


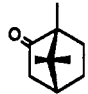
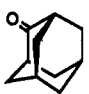

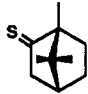
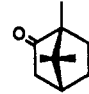
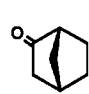

FIGURE 4: Comparison of the two different binding orientations determined crystallographically for thiocamphor. The presence of the distal ligand is only compatible sterically with the minor (30%) orientation shown on the right.

sulfur atom: positive between the substrate and porphyrin ring; negative between the substrate and distal helix. Since a rotation of the sulfur to better accommodate this residual density resulted in a much deteriorated fit of the thiocamphor methyl groups to the electron density, we attempted to fit thiocamphor to the density in yet a third orientation. This orientation again had the sulfur directed toward the heme, but now the six-membered ring of the substrate was essentially parallel to the porphyrin plane (Figure 4B), rather than perpendicular as it had been previously (and as it is when camphor binds). The new  $F_o - F_c$  map based on this thiocamphor orientation had considerable difference electron density, indicating that this was not the major binding orientation of thiocamphor.

Finally, we were best able to minimize the difference electron density by including thiocamphor in both orientations (Figure 4), neither corresponding to that of camphor. The occupancy of the first orientation was estimated and fixed at 70%. In this position the sulfur atom approaches to within 2.35 Å of the distal ligand and most likely displaces it. The occupancy of the second orientation was fixed at 30%, and in this position the sulfur atom is 3.80 Å from the distal ligand. Curiously enough, when the occupancy of the distal ligand was fixed at 0.30 (to correspond with the second thiocamphor orientation) and only its temperature factor allowed to refine, although the temperature factor dropped to quite a low value (10 Å<sup>2</sup>), positive difference density still remained around this ligand in  $F_o - F_c$  maps. Nor did subsequent release of the fixed occupancy of the distal ligand, during refinement, remove the difference density, despite the fact that the occupancy climbed to 0.51 (after 20 refinement cycles; the temperature factor also dropped to 8.3 Å<sup>2</sup> during this time). These results suggest that occupancies and temperature factors are unable to recover, in a reasonable number of refinement cycles, from initial poor estimates of these values. They also confirm that though highly correlated, occupancies and temperature factors are not entirely interchangeable as modeling parameters.

We were only able to eliminate the difference electron density from around the distal ligand by including it initially with full occupancy and a temperature factor of 20.0 Å<sup>2</sup>, near the mean temperature factor for all protein and heme atoms, and allowing both occupancy and temperature factor of this ligand to refine. In the final model, the distal ligand has a temperature factor of 19.6 Å<sup>2</sup> and an occupancy of 0.90 and  $F_o - F_c$  maps calculated with these coordinates show no residual difference density around the sixth ligation position. The temperature factor of thiocamphor itself refined to about 23.5 Å<sup>2</sup>, or about 50% higher than that of camphor bound in the active site. This higher mobility for thiocamphor, a larger substrate than camphor, suggests that thiocamphor may occupy additional minor orientations, possibly the one corresponding to camphor bound to the enzyme. Minor thiocamphor orientations which we have not modeled could potentially account also for the discrepancy between the occupancies of the distal ligand and of thiocamphor orientation 2 (Figure 4B). Another influential feature could be the fact that

Table III: Various Substrate-Dependent Parameters<sup>a</sup>

							
	camphor	admantanone	adamantane	thiocamphor	camphor/Y96F	norcamphor	camphane
molec vol	315 Å <sup>3</sup>	300 Å <sup>3</sup>	293 Å <sup>3</sup>	322 Å <sup>3</sup>	315 Å <sup>3</sup>	236 Å <sup>3</sup>	309 Å <sup>3</sup>
hydrogen bond to Y96	yes <sup>a</sup>	yes <sup>b</sup>	no	no	no	yes <sup>b</sup>	no
no. of iron ligands	5 <sup>a</sup>	5 <sup>b</sup>	6	6		6 <sup>b</sup>	6
redox pot. Fe <sup>3+</sup> /Fe <sup>2+</sup>	-170 mV <sup>c</sup>	-175 mV <sup>c</sup>				-206 mV <sup>c</sup>	
high-spin %	94-97% <sup>c,e</sup>	96-98% <sup>c,d</sup>	99% <sup>d</sup>	65% <sup>e</sup>	59% <sup>e</sup>	46% <sup>c</sup>	46% <sup>e</sup>
regiospecif of substr hydroxylatn	5-exo (100%) <sup>d,f</sup>	5 (100%) <sup>d</sup>	1 (100%) <sup>d</sup>	5-exo (64%) <sup>e</sup> 6-exo (34%) 3-exo (2%)	5-exo (92%) <sup>e,f</sup> 4 (1%) 6-exo (2-4%) 3-exo (0-4%) 9 (<1%)	5-exo (45%) <sup>f</sup> 6-exo (47%) 3-exo (8%)	5-exo (90%) <sup>e</sup> 6-exo (10%)
substr temp factor (Fe <sup>3+</sup> )	16.2 Å <sup>2a</sup>	16.5 Å <sup>2b</sup>	24.7 Å <sup>2</sup>	23.5 Å <sup>2</sup>		33.5 Å <sup>2b</sup>	30.1 Å <sup>2</sup>
substr hydrophilic groups	yes	yes	no	yes	yes	yes	no
hydroxylatn "efficiency"	100% <sup>e,f</sup>			98% <sup>e</sup>	100% <sup>e</sup>	12% <sup>f</sup>	8% <sup>e</sup>
L6-substr dist	NA	NA	2.63 Å	2.35 Å (70%) 3.35 Å (30%)		3.0 Å <sup>b</sup>	2.88 Å
L6-iron dist	NA	NA	1.95 Å	1.35 Å		1.73 Å <sup>b</sup>	1.67 Å
L6 occupancy	NA	NA	1.00	0.90		0.97 <sup>b</sup>	1.00
L6 temp factor	NA	NA	14.3 Å <sup>2</sup>	19.6 Å <sup>2</sup>		3.8 Å <sup>2b</sup>	7.7 Å <sup>2</sup>
cation occupancy	1.00 <sup>a</sup>	1.00 <sup>b</sup>	0.89	0.91		1.00 <sup>b</sup>	0.72
cation temp factor	12.1 Å <sup>2a</sup>	10.0 Å <sup>2b</sup>	15.5 Å <sup>2</sup>	14.2 Å <sup>2</sup>		7.9 Å <sup>2b</sup>	21.7 Å <sup>2</sup>

<sup>a</sup> Poulos et al. (1985, 1987). <sup>b</sup> Raag and Poulos (1989a). <sup>c</sup> Fisher and Sligar (1985). <sup>d</sup> White et al. (1984). <sup>e</sup> Atkins and Sligar (1988b). <sup>f</sup> Atkins and Sligar (1989). <sup>g</sup> Carbon numbering for each substrate begins with C-1 at the top of the six-membered ring which is in the plane of the table. Numbering proceeds counterclockwise such that the carbonyl carbon is C-2 and C-5 is in the lower right-hand portion of the ring. Note that C-5 is a secondary carbon in some substances and a tertiary carbon in others.

the distal ligand is located between the heme iron and the substrate sulfur atom. These two neighbors could conceivably interact via the distal ligand and increase electron density at this location, which could be reflected in an anomalously high ligand occupancy.

Although initial occupancy estimates for the two thiocamphor orientations were successful in eliminating substrate-associated difference electron density, we decided to explore other occupancy combinations because of the discrepancy between the refined occupancy of the distal ligand (0.90) and the estimated occupancy of the thiocamphor orientation (0.30), which would be sterically compatible with the presence of the ligand. After calculating and examining maps based on occupancy combinations ranging from 0.30/0.70 to 0.80/0.20 in increments of 0.10, we concluded that the relative occupancies of thiocamphor orientations 1 and 2 (parts A and B of Figure 4, respectively) are probably around 65% and 35%, respectively, with an error of roughly 10%.

## DISCUSSION

### Substrate Hydroxylation Profiles

**Camphane.** Although camphane is incapable of hydrogen bonding with Tyr96, its similarity to camphor in overall shape and size causes it to be bound in a nearly identical position in the P-450<sub>CAM</sub> active site. The methyl groups of camphane and camphor interact with the same active site features. As with camphor, the 5-carbon atom of camphane is the nearest to the heme iron atom, explaining the observed preference (90% of products) for 5-exo hydroxylation of this substrate (Atkins & Sligar, 1988b). That 10% of the products are 6-exo hydroxylated (Atkins & Sligar, 1988b) can be attributed to the enhanced mobility of camphane in the P-450<sub>CAM</sub> active site (Table III).

Hydroxylation profiles and crystallographic data on norcamphor- and camphane-P-450<sub>CAM</sub> complexes, in comparison with camphor complexes, demonstrate that two features, a hydrogen bond to the enzyme and complementary van der

Waals interactions, are both necessary to lower the mobility of a substrate. Low substrate mobility, as revealed by crystallographic temperature factors, appears to be critical for high regiospecificity of substrate metabolism (Table III).

**Adamantane.** Adamantane is the only substrate we have investigated, in this study, that is metabolized to a single product despite having a relatively high active site mobility. The single product can be attributed to the existence of only two types of unique carbon atoms in adamantane, together with the greater reactivity of tertiary versus secondary carbons (White et al., 1984).

**Thiocamphor.** Thiocamphor binds to P-450<sub>CAM</sub> in two orientations, both of which are different from that preferred by camphor and both of which have sulfur as the substrate atom nearest to iron. A priori, the proximity of the sulfur atom to the heme suggests that the thiocamphor hydroxylation mechanism might involve an initial single electron transfer from sulfur to heme instead of, or in competition with, initial hydrogen abstraction, as is thought to occur with camphor (Ortiz de Montellano, 1986). However, the major products of thiocamphor metabolism are 5- and 6-exo hydroxylated, and these substrate atoms are among the farthest substrate atoms from the active oxygen location in our thiocamphor-P-450<sub>CAM</sub> model. Modeling of thiocamphor in the orientation preferred by camphor (with full occupancy) resulted in difference electron density maps strongly suggesting that such a model was incorrect. Nevertheless, the products of thiocamphor hydroxylation imply that this substrate is only metabolized when it adopts a camphor-like orientation in the active site. These data lead us to conclude that the conformers seen in the crystal structure are nonproductive and that the camphor-like conformer is fractionally occupied and crystallographically unobservable. Although thiocamphor appears to make a snug van der Waals fit with P-450<sub>CAM</sub>, it may be possible for it to occasionally rotate within the active site to yield a camphor-like complex, as suggested by molecular dynamics simulations of the Tyr96Phe mutant-camphor complex

(Richard Ornstein and Mark Paulsen, personal communication).

### *Distal Aqua Ligand (L6)*

Camphor and adamantanone both have low temperature factors and displace the distal ligand, while all of the other substrates investigated here are more loosely bound and do not displace the ligand. As with norcamphor (Raag & Poulos, 1989a), the distal ligand in the presence of camphane has full occupancy and a very low temperature factor ( $7.7 \text{ \AA}^2$ ), indicating that the 46% high-spin percentage of the camphane-bound enzyme is probably not due to partial occupancy of the distal ligation site. Rather, by displacing most of the active site solvent of the substrate-free enzyme (Poulos et al., 1986), camphane increases the active site hydrophobicity, thereby shifting the  $\text{OH}^-/\text{H}_2\text{O}$  equilibrium toward  $\text{H}_2\text{O}$  and yielding an increase in redox potential. Partial protonation of the distal ligand decreases its ligand field strength, which is responsible for the increase in high-spin percentage. This argument is supported by the observation that only high-spin P-450<sub>CAM</sub> is protonated (Sligar & Gunsalus, 1979).

The adamantane-P-450<sub>CAM</sub> complex is especially interesting because, although the small size and relatively high mobility of this substrate allow the heme to remain hexacoordinate, this complex is fully high-spin like the pentacoordinate camphor- and adamantanone-P-450<sub>CAM</sub> complexes (Table III). There are two factors that could account for the high-spin nature of the adamantane complex: a relatively long Fe-L6 distance and a high distal ligand mobility (Table III). Of all the substrate-P-450<sub>CAM</sub> structures we have determined, the iron-sixth ligand distance is at its longest ( $1.96 \text{ \AA}$ ) in the presence of adamantane. Both the long bond length and greater ligand mobility could result from the relatively close approach of adamantane to the distal ligand: approximately  $0.4 \text{ \AA}$  closer than norcamphor or camphane. This short substrate-ligand distance may also promote protonation of the ligand, resulting in the observed high-spin hexacoordinate complex.

Thiocamphor does not fit the shorter iron-L6 distance/lower spin pattern. It induces a spin state (65% high spin) intermediate between those induced by norcamphor and camphane (46%) and adamantane (100%), but in the presence of thiocamphor the iron-L6 distance is only  $1.35 \text{ \AA}$ , the shortest we have seen. However, the thiocamphor complex is not directly comparable to the other substrate complexes since at least two orientations are observable. It may be that a population in which thiocamphor bound exclusively in the ligand-allowing orientation (Figure 4b) would have a greater low-spin component than the 65% quoted in Table III, which presumably arises from a population with mixed binding modes. In addition, in the presence of thiocamphor the distal ligand appears to be linking iron and the substrate sulfur atom and its ligand field strength may thus be different from that of a simple  $\text{OH}^-/\text{H}_2\text{O}$  ligand.

A final point regarding the almost unbelievably short iron-L6 distance in the presence of thiocamphor should be made. Recall that only the minor crystallographically observed thiocamphor orientation is sterically compatible with the presence of a distal ligand. However, the electron density against which our model is refined represents contributions from all thiocamphor orientations in all protein molecules in the crystal lattice. This averaged electron density, which for the most part lacks a distal ligand contribution, probably obscures the real distal ligand position in the minor orientation, resulting in the anomalously short iron-L6 distance observed.

Distal ligand movement, not iron movement, appears re-

sponsible for differences in the iron-ligand distance. The ligand location changes by about  $0.6 \text{ \AA}$  in the presence of different substrates. Iron and proximal cysteine positions are quite static, despite the large changes in spin equilibrium associated with these three substrates. Although iron-distal ligand and iron-cysteine sulfur (proximal ligand) distances changed very little ( $0.03\text{--}0.05 \text{ \AA}$ ) as a result of unrestrained refinement, multiple substrate orientations as well as incomplete substrate occupancies may have resulted in somewhat artifactual distal ligand positions and distal ligand related distances.

### *Cation Site and Non-Hydrogen-Bonding Substrates*

In considering the various parameters interrelating substrate binding, spin state, and redox potential, the role of cations is important. Cations stabilize high-spin, substrate-bound P-450<sub>CAM</sub> (Peterson, 1971; Lange & Debey, 1979; Lange et al., 1979; Hui Bon Hoa & Marden, 1982; Fisher et al., 1985; Hui Bon Hoa et al., 1989). Poulos et al. (1987) identified a potential cation binding site most likely responsible for these effects. The presumed cation is octahedrally coordinated by two solvent molecules and by four carbonyl oxygens, including that of Tyr96 (Poulos, 1987; Poulos et al., 1987). The cation appears to stabilize a rather unusual conformation for the tyrosine, which occurs at the end of a helix. Further support for the role of this cation site as the one responsible for stabilizing the high-spin state stems from recent mutagenesis studies (Di Primo et al., 1990). Conversion of Tyr96 to phenylalanine significantly decreases the ability of potassium ions to convert P-450<sub>CAM</sub> to the high-spin state.

An interesting feature (Table III) of all of the structures we have determined in which the substrate does not hydrogen bond with Tyr96 (camphane, adamantane, and thiocamphor) is that the temperature factor and occupancy of the cation are higher and lower, respectively, than in structures with hydrogen-bonding substrates (camphor, adamantanone, and norcamphor). In the presence of camphane, the occupancy of the cation (0.72) is even lower than it is in the substrate-free enzyme (0.91; Poulos et al., 1986). The temperature factors of the six cationic ligands also are higher in the absence of an enzyme-substrate hydrogen bond. These results, together with the known cation stabilization of P-450<sub>CAM</sub>, suggest that the enzyme is generally more stable in the presence of hydrogen-bonding than non-hydrogen-bonding substrates. Thus by hydrogen bonding to Tyr96 (or by forming nonbonded interactions near Tyr96), substrates may enhance enzyme stability via cation occupancy and mobility, which may indirectly induce subtle global conformational changes in the enzyme.

### *Uncoupling*

In camphor hydroxylation by P-450<sub>CAM</sub>, 100% of NADH consumed is channeled toward 5-*exo*-hydroxycamphor production. That is, camphor hydroxylation by P-450<sub>CAM</sub> proceeds with 100% efficiency. However, the efficiency drops to only 12% and 8% when norcamphor and camphane, respectively, are metabolized (Table III). Norcamphor and camphane are "uncouplers" of P-450<sub>CAM</sub> metabolism (Figure 1) and promote the enzyme to produce hydrogen peroxide and/or water rather than hydroxylated substrate (Staudt et al., 1974; Zhukov & Archakov, 1982; Gorsky et al., 1984; Atkins & Sligar, 1987, 1988a). Substrates may also induce spontaneous decay of ferrous  $\text{O}_2$ -P-450<sub>CAM</sub>, leading to enzyme autoxidation (Eisenstein et al., 1977).

Clearly, uncoupling cannot be a simple function of the absence of either complementary enzyme-substrate interactions or of an enzyme-substrate hydrogen bond, as both norcamphor



and camphane uncouple P-450<sub>CAM</sub> metabolism. Uncoupling may occur even when the cation site has a low temperature factor and full occupancy, as seen with norcamphor-P-450<sub>CAM</sub>. Uncoupling is not strictly related to high or low regiospecificity of substrate metabolism. Nor does it appear to be related solely to the fraction of low-spin heme or presence of the distal ligand since thiocamphor hydroxylation occurs with 98% efficiency (Table III). However, since the thiocamphor-P-450<sub>CAM</sub> complex may be nonproductive, it would be interesting to know if thiocamphor in a camphor-like orientation displaces the distal ligand.

**Substrate Mobility and Uncoupling.** Norcamphor and camphane do have common features, which may account for their inefficient hydroxylation by P-450<sub>CAM</sub>. One of these is that both substrates exhibit high mobility in the active site, with similar average atomic temperature factors of 33.5 and 30.1 Å<sup>2</sup>, respectively. These high mobilities are attributable to the same factors that cause loss of hydroxylation regiospecificity, the lack of a complementary fit between enzyme and substrate in one case and the lack of an enzyme-substrate hydrogen bond in the other, suggesting that uncoupling could have multiple proximal causes. Although substrate mobility may be somehow correlated with uncoupling, the relationship cannot be linear. Judging from even the small number of substrates with known hydroxylation efficiencies (Table III), it is rather curious that there are none that are metabolized with intermediate efficiencies; they are all either "good" or "bad" substrates. The relative mobilities of substrates bound to P-450<sub>CAM</sub> suggest that there may exist some kind of mobility threshold above which uncoupling occurs.

**Substrate Hydrophilic Groups, Uncoupling and Catalysis.** Besides orienting the substrate and helping to lower substrate mobility, the Tyr96-substrate hydrogen bond may have another role. In the CO-camphor-P-450<sub>CAM</sub> structure (Raag & Poulos, 1989b), we observed that carbon monoxide pushes camphor by nearly a full angstrom toward the putative substrate access channel (Poulos et al., 1986), although the camphor carbonyl oxygen-Tyr96 hydrogen bond is preserved. On the basis of the ferrous CO-camphor-P-450<sub>CAM</sub> structure, we expect that when O<sub>2</sub> binds, it will also push substrates "up" away from the heme. Following cleavage of the dioxygen bond and departure of the terminal oxygen, the substrate should have room to return toward the now activated and single, iron-linked oxygen atom. This process may depend on the existence of a hydrogen bond between Tyr96 and the substrate. We thus propose that beyond orienting a substrate and reducing its mobility, the active site tyrosine may act as a "restoring force" to facilitate substrate return toward the hydroxylating species. If a substrate did not return toward the catalytic oxygen-iron species, one might anticipate uncoupling of the P-450 reaction, with reduction of the iron-linked oxygen to water or hydrogen peroxide rather than substrate oxidation. Camphane (and adamantane?) may be such an effective uncoupler because it gets "stuck" in or near the hydrophobic access channel and is unable to return toward the active oxygen intermediate following cleavage of the dioxygen bond.

**Ultimate Cause of Uncoupling.** Uncoupling may be related to substrate mobility (norcamphor, camphane, adamantane?), hydrophobicity (camphane, adamantane?), the distance of a substrate from the active oxygen location, or some combination of these factors. However, regardless of the initial cause in any specific case, the primary factor causing the switch from monooxygenase to oxidase activity is probably the presence of extra solvent, in addition to the distal ligand, around the

dioxygen bond undergoing cleavage. Solvent in the active site during catalysis would provide a source of protons that could facilitate dioxygen dissociation as hydrogen peroxide and/or dioxygen cleavage and reduction to water (Atkins & Sligar, 1987). Thus, in cases in which a substrate is highly mobile, or is not close enough to the heme, uncoupling may be favored over productive metabolism.

**Evidence for Active Site Solvent in the Presence of Uncouplers.** That discrete "extra" water molecules are not evident in either camphane-P-450<sub>CAM</sub> or norcamphor-P-450<sub>CAM</sub> electron density maps is not overly troublesome as both substrates are highly mobile. Active site solvent not strongly hydrogen bonded to protein or substrate may be severely disordered and unobservable. In fact, randomly ordered, mobile active site solvent in the presence of norcamphor and camphane could itself be one factor driving the temperature factors of these substrates to such high values during refinement.

We do, however, have evidence that *disordered* solvent may be in the active site together with some substrates. In electron density maps of both camphane- and adamantane-P-450<sub>CAM</sub> complexes, an internal solvent molecule (water 687) that is normally located "behind" the distal helix on the side away from the active site is missing (in  $2F_o - F_c$  maps when contoured above approximately 0.25–0.30 $\sigma$ ) (Figure 5A,B). Solvent 687 is present in all other structures we have determined, including thiocamphor-P-450<sub>CAM</sub>, which also lacks an enzyme-substrate hydrogen bond (Figure 5C). As shown schematically in Figure 6, water 687 is part of an internal solvent channel connecting Thr252 with the buried residue Glu366. In the presence of camphor, this internal solvent pocket contains three crystallographically ordered solvent molecules. Glu366 is found in 42 of 53 sequences aligned by Nelson and Strobel (1989) and is part of the proximal helix (helix L), which is one of the most highly conserved segments in all P-450s. Therefore, this unusual structural feature with ordered solvent situated between a key active site residue (Thr252) and a buried glutamate side chain may be a structural feature shared by many P-450s. Unlike peroxidases where suitably positioned charged and acid-base side chains serve as catalytic groups for heterolytic O–O bond cleavage (Poulos & Finzel, 1984), P-450<sub>CAM</sub> has no similar set of residues, leaving water as the main candidate for a proton source. The solvent pocket linking Thr252 and Glu366 may serve this function.

Water 687 is missing not only in the presence of camphane and adamantane but also in the substrate-free P-450<sub>CAM</sub> structure. This suggests that, as the natural substrate camphor enters through the proposed access channel (Poulos et al., 1986), it may push at least one active site solvent molecule farther into the active site, toward and over the distal helix and into the water 687 location. Since the water 687 site is unoccupied in the presence of camphane and adamantane, one might expect electron density corresponding to an active site solvent molecule somewhere between these substrates and the water 687 site, near the distal helix.

This is an interesting possibility because in camphane-P-450<sub>CAM</sub>, adamantane-P-450<sub>CAM</sub>, and substrate-free P-450<sub>CAM</sub> maps, there is positive  $F_o - F_c$  difference electron density at 3 $\sigma$  near Thr252 and Gly248, the highly conserved (Nelson & Strobel, 1989) distal helix residues that form the putative dioxygen binding groove (Figure 5D,E). The difference density is too close to the helix to be accounted for by hydrogen-bonded water. There is also no corresponding negative density to indicate that major side-chain rearrangements have occurred.

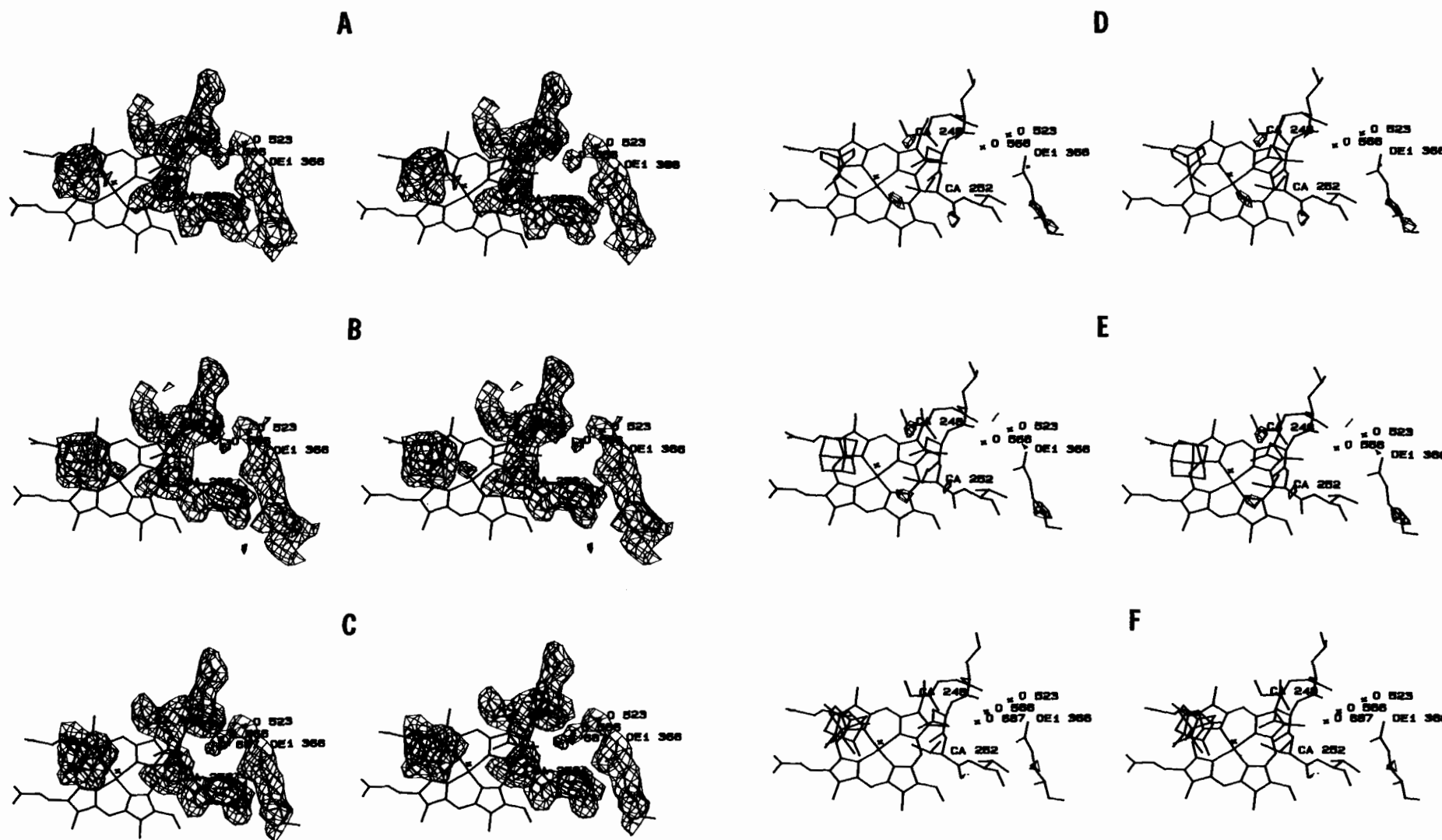


FIGURE 5: Final  $2F_o - F_c$  (A–C, contoured at  $+1\sigma$ ) and  $F_o - F_c$  (D–F, contoured at  $+3\sigma$ ) electron density maps for camphane– (A, D), adamantane– (B, E), and thiocamphor– (C, F) P-450<sub>CAM</sub> complexes. There is no significant negative ( $-3\sigma$ )  $F_o - F_c$  density in the regions contoured. The view is looking along the heme normal or rotated by about  $90^\circ$  around the horizontal axis from the view used in other figures. Substrates are on the left of the figure, the distal ligand is denoted by a cross near the heme iron, and the dioxxygen binding region of the distal helix appears on the right. On the non active site side of the distal helix is the buried solvent channel shown schematically in Figure 6. This solvent channel leads from the distal helix and Thr252 to Glu366 via three water molecules (numbered 687, 566, and 523). Note the presence of  $F_o - F_c$  density near Gly248 and

Thr252 (top and bottom of the dioxxygen binding groove, respectively) in camphane (D) and adamantane (E)  $F_o - F_c$  maps but not in the thiocamphor (F)  $F_o - F_c$  map. We attribute this positive  $F_o - F_c$  density to disordered solvent in the active site in the presence of camphane and adamantane. Note also the  $2F_o - F_c$  density corresponding to Wat687 (on the nonactive site side of distal helix) in the thiocamphor (C) map but missing in camphane (A) an adamantane (B)  $2F_o - F_c$  maps. Water 687 may play a role in uncoupling P-450<sub>CAM</sub> metabolism by moving over the distal helix to provide a proton source for hydrogen peroxide and water production. Val253 is located on the “back” of the distal helix near the water 687 location. Mutation of Val253 to threonine or serine in P-450<sub>CAM</sub> might protect this enzyme against uncoupling.



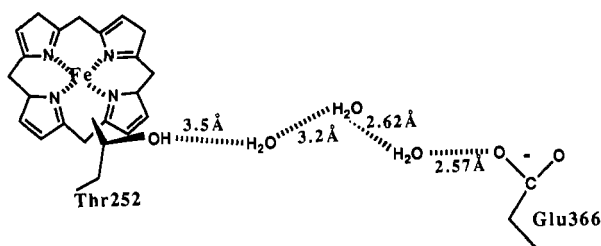


FIGURE 6: Schematic depiction of the solvent channel between Thr252 and Glu366 containing internal solvent molecules 523, 566, and 687 (Poulos et al., 1987). These solvent molecules, as well as Glu366, are completely enclosed by protein from the active site as well as from bulk solvent.

Thus *disordered* water may exist near the dioxygen binding groove in adamantane-P-450<sub>CAM</sub>, camphane-P-450<sub>CAM</sub>, and substrate-free P-450<sub>CAM</sub>. Moreover, in most structures in which water 687 is present, residual positive difference density is *not* observed or is essentially negligible around Gly248 and Thr252 (Figure 5F).

That water 687 is present "behind" the distal helix in the norcamphor-P-450<sub>CAM</sub> structure but not in camphane-bound P-450<sub>CAM</sub> might suggest that its presence or absence is not related to uncoupling. However, temperature factors of Gly248 and Thr252 atoms are on the order of 40% higher (5–6 Å<sup>2</sup>) in camphane-, adamantane-, and norcamphor-bound P-450<sub>CAM</sub> than they are in other substrate complexes. (In the substrate-free enzyme, the temperature factors of Gly248 atoms are even higher.) Thus, disordered active site solvent also may be present with norcamphor. The fact that the atomic temperature factors are so much higher near this proposed disordered solvent supports its existence. Temperature factors of protein atoms could refine to higher values to account for neighboring density, which has not been included in an atomic model.

Water 687 may be involved in uncoupling of P-450<sub>CAM</sub> substrate metabolism. Substrates with high mobility in the active site such as norcamphor and camphane may jostle iron-bound dioxygen, causing it to adopt alternate orientations. This hypothesis is supported by multiple infrared CO stretching modes in P-450<sub>CAM</sub> (Jung & Marlow, 1987) as well as by the ferrous CO-camphor-P-450<sub>CAM</sub> structure (Raag & Poulos, 1989b). When we allowed occupancies of carbon monoxide atoms to refine, the lower occupancy of oxygen (0.8) than of carbon (1.0) suggested that even in the presence of camphor, diatomic ligands may not be confined to a single orientation. If and when dioxygen is not directed toward the Gly248–Thr252 helical groove, a solvent molecule may bind there, facilitating uncoupling. Note that in its internal binding site, water 687 forms about 10 contacts with neighbors under 3.5 Å distant, including ones with three amide nitrogens, two carbonyl oxygens, the side-chain hydroxyl of Thr252, and another internal water molecule (water 566). We do not know the energy barrier for displacement of water 687 but the groove on the "back side" of the distal helix in which water 687 is bound appears to shrink slightly when water 687 is absent. Subtle global conformational changes of the protein, associated with binding of uncoupling substrates, could force the water 687 binding site to contract, effectively ejecting this molecule into the active site, resulting in uncoupling. Of course, the disordered active site solvent does not necessarily have to be water 687, although the solvent channel between Thr252 and Glu366 containing water 687 is the nearest solvent source to the active site.

**Mutation-Induced Uncoupling of P-450s.** Finally, not only do some metabolizable compounds uncouple P-450 substrate

oxygenation, but certain mutations of the enzyme have similar effects. Several amino acids that are predicted to occur in all P-450s in the active site region, based on the structure of P-450<sub>CAM</sub> (Poulos et al., 1985, 1986), are highly conserved (Nelson & Strobel, 1988, 1989; Gotoh & Fujii-Kuriyama, 1989). Two of these, Gly249 and Thr252 (numbering according to P-450<sub>CAM</sub>), are both invariant among at least 51 P-450 sequences (Nelson & Strobel, 1989). In P-450<sub>CAM</sub> they are located in the distal helix and may influence substrate specificity and/or oxygen activation during catalysis (Poulos et al., 1985, 1987). The highly conserved threonine is in contact with carbon monoxide in ferrous CO-camphor-P-450<sub>CAM</sub> (Raag & Poulos, 1989b) and due to its polar character probably stabilizes iron-bound dioxygen (Collman et al., 1980). Mutations of the active site Thr residue can cause uncoupling of P-450 reactions (Imai et al., 1989; Martinis et al., 1989). Imai et al. (1989) have suggested that Thr252 of P-450<sub>CAM</sub> might serve as a proton donor to the iron-linked oxygen to facilitate O–O bond cleavage. However, we doubt that a side-chain OH group with such a high pK would operate as an acid catalyst. The finding that the Thr252Val mutant allows O<sub>2</sub> cleavage to occur, producing more water than observed with any other mutant, casts further doubt on Thr252 as a proton donor (Imai et al., 1989). Water production, unlike the generation of hydrogen peroxide, depends on the cleavage of the O–O bond. Thus, it appears more likely that the role of Thr252 is structural.

Mutation-induced uncoupling of P-450 substrate oxygenation could be caused by distortions in the oxygen binding site that destabilize oxygen, causing it to dissociate, and/or by increasing accessibility of the active site to solvent, perhaps via the buried solvent channel between Thr252 and Glu366 (Figure 6). We propose that the way in which mutations of the invariant threonine to valine or alanine promote uncoupling is as follows. In wild-type P-450<sub>CAM</sub>, dioxygen is electrostatically stabilized by Thr252 (Collman et al., 1980; Raag & Poulos, 1989b), one of the few hydrophilic active site groups. Mutation of this residue to a hydrophobic one destabilizes the major dioxygen binding orientation and allows the ligand more freedom of movement in the active site. Destabilization also occurs because the hydrogen bond between the Thr252 side-chain OH group and the carbonyl oxygen atom of Gly248, which helps to form part of the O<sub>2</sub> site, is disrupted. That hydrogen bonding is important in stabilizing the oxy complex is evidenced by the Thr252Ser mutant, which has nearly full wild-type efficiency (Imai et al., 1989) presumably because serine is capable of the same hydrogen bonding interactions as threonine. With the distal helix groove between Gly248 and Thr252 no longer dominated by dioxygen, there may be room for water 687 or another solvent molecule to bind in this region. On the active site side of the distal helix, there are few potential interactions that could strongly bind a solvent molecule. Thus its binding location may encompass the entire dioxygen binding groove region, from Gly248 to the residue at the 252 location and perhaps beyond, accounting for the disordered quality of the density we attribute to this water molecule. If dioxygen spends less time directed toward the distal helix, not only may it allow solvent to enter the dioxygen binding groove but it may itself sterically interfere with the approach of substrate toward the heme, facilitating uncoupling.

Whether dioxygen dissociates as peroxide or is cleaved and reduced to water appears to depend on the specific mutation (Imai et al., 1989). That different P-450 mutants have different high- and low-spin fractions (Imai & Nakamura, 1989) supports the idea that these mutants have varying active site

solvent accessibilities. Some substrates also appear to be more sensitive than others to P-450 active site mutations (Furuya et al., 1989a,b), a phenomenon that appears to be related to conformational flexibility of the substrate.

**A Residue That May Protect against Uncoupling.** In 36 of 52 P-450 sequences that have been aligned (Nelson & Strobel, 1989), the sequence Thr-Thr replaces Thr-Val (252–253) in P-450<sub>CAM</sub>. Residue 253 of P-450<sub>CAM</sub>, immediately downstream of the invariant threonine, is located on the “back” of the distal helix in a position in which it should be able to hydrogen bond to water 687, if it were a threonine or serine. A residue capable of hydrogen bonding to water 687 on the back of the distal helix could protect P-450s against uncoupling, at least when and if uncoupling is mediated via this water molecule. In mutagenesis experiments with different P-450s, hydrogen peroxide and water production (resulting from uncoupling) should be monitored in addition to catalytic activities to explore this issue. If water 687 plays a role in uncoupling it is likely that (1) a Thr (corresponding to 253 in P-450<sub>CAM</sub>) may yield an enzyme more resistant to uncoupling induced by mutations of the immediately preceding, invariant threonine and (2) a Thr-Thr sequence (corresponding to 252–253 in P-450<sub>CAM</sub>) may be more resistant to substrate-induced uncoupling than a Thr-Val sequence in this location.

In this light, a report from the 1990 Microsomes and Drug Oxidations VIII meeting in Stockholm, Sweden, is very intriguing. Imai and colleagues observed lower laurate and caprate hydroxylase activities with a Thr-Val sequence than with Thr-Ser or Thr-Thr sequences in chimeric P450s, although they did not monitor peroxide or “excess” water production (Imai et al., 1990).

## CONCLUSIONS

Hydroxylation profiles of norcamphor and camphane by P-450<sub>CAM</sub> demonstrate that both a complementary fit between substrate and enzyme and a hydrogen bonding “anchor” between substrate and enzyme are essential to orient and bind the substrate tightly in order to obtain the absolute regio- and stereospecificity observed with camphor hydroxylation (Atkins & Sligar, 1988b, 1989). Our crystallographic results show that high mobility and loss of specificity are strongly correlated.

Distal ligand displacement by a substrate may also depend on the mobility-lowering effect of an enzyme–substrate hydrogen bond, as demonstrated by comparison of camphor/camphane and adamantanone/adamantane temperature factors (Table III). Hydrogen bonding between enzyme and substrate, in turn, lowers the mobility and increases the occupancy of the cation site, which results in enhanced stability of the enzyme in the presence of hydrogen-bonding substrates (Hui Bon Hoa et al., 1989; Di Primo et al., 1990).

Whether or not the distal aqua ligand remains in a substrate–P-450 complex is controlled by steric crowding between the substrate and ligand, and is influenced by both substrate size and mobility. Moreover, the high/low spin equilibrium is controlled not only by the presence or absence of the aqua ligand but also by the state of distal ligand protonation (Sligar & Gunsalus, 1979). Based on the adamantane complex, P-450<sub>CAM</sub> can remain hexacoordinate yet be fully high-spin due to the high mobility of the aqua ligand and the long Fe–L6 distance. High L6 mobility and long Fe–L6 distance result from the close approach of adamantane to the aqua ligand, which may also increase the proton affinity of the ligand.

Disordered solvent is present in the active site in the presence of highly mobile substrates. This active site water(s) may be directly responsible for uncoupling, the diversion of reducing

equivalents away from substrate hydroxylation and toward hydrogen peroxide and/or water production. We have identified an internal solvent molecule, water 687, located on the opposite side of the distal helix from the dioxygen-binding groove, which does not appear to be present in all substrate–P-450<sub>CAM</sub> complexes and which may be associated with uncoupling. We propose that P-450s in which the residue immediately downstream of the invariant active site threonine is also a threonine, or a serine, may resist uncoupling by providing an additional hydrogen bond to water 687 and thereby stabilizing it in its nonactive site location.

Water 687 is part of an internal solvent pocket between two highly conserved residues, Thr252 in the active site and the buried side chain of Glu366. This solvent channel may serve as the source of protons required in cleaving the O–O bond during the P-450 catalytic cycle.

## ACKNOWLEDGMENTS

R.R. is especially indebted to Pat Alexander and Phil Bryan for assistance in thiocamphor synthesis. We also thank Richard Ornstein and Mark Paulsen for permission to quote molecular dynamics results prior to publication.

## REFERENCES

- Anders, M. W., Ed. (1985) *Bioactivation of Foreign Compounds*, Academic Press, Inc., New York.
- Atkins, W. M., & Sligar, S. G. (1987) *J. Am. Chem. Soc.* 109, 3754–3760.
- Atkins, W. M., & Sligar, S. G. (1988a) *Biochemistry* 27, 1610–1616.
- Atkins, W. M., & Sligar, S. G. (1988b) *J. Biol. Chem.* 263, 18842–18849.
- Atkins, W. M., & Sligar, S. G. (1989) *J. Am. Chem. Soc.* 111, 2715–2717.
- Bernstein, F. C., Koetzle, T. F., Williams, G. J. B., Meyer, E. F., Jr., Brice, M. D., Rogers, J. R., Kennard, O., Shimanouchi, T., & Tasumi, M. (1977) *J. Mol. Biol.* 112, 535–542.
- Collman, J. P., Halbert, T. R., & Suslick, K. S. (1980) in *Metal Ion Activation of Dioxygen* (Spero, T. G., Ed.) pp 1–72, John Wiley & Sons, New York.
- Debrunner, P. G., Gunsalus, I. C., Sligar, S. G., & Wagner, G. C. (1978) in *Metals in Biological Systems* (Sigel, H., Ed.) Vol. 7, pp 241–275, Marcel Dekker, New York.
- Demarco, P. V., Doddrell, D., & Wenkert, E. (1969) *Chem. Commun.*, 1418–1420.
- Di Primo, C., Hui Bon Hoa, G., Douzou, P., & Sligar, S. (1990) *J. Biol. Chem.* 265, 5361–5363.
- Eisenstein, L., Debey, P., & Douzou, P. (1977) *Biochem. Biophys. Res. Commun.* 77, 1377–1383.
- Fisher, M. T., & Sligar, S. G. (1985) *J. Am. Chem. Soc.* 107, 5018–5019.
- Fisher, M. T., Scarlata, S. F., & Sligar, S. G. (1985) *Arch. Biochem. Biophys.* 240, 456–463.
- Furuya, H., Shimizu, T., Hirano, K., Hatano, M., Fujii-Kuriyama, Y., Raag, R., & Poulos, T. L. (1989a) *Biochemistry* 28, 6848–6857.
- Furuya, H., Shimizu, T., Hatano, M., & Fujii-Kuriyama, Y. (1989b) *Biochem. Biophys. Res. Commun.* 160, 669–676.
- Gorsky, L. D., Koop, D. R., & Coon, M. J. (1984) *J. Biol. Chem.* 259, 6812–6817.
- Gotoh, O., & Fujii-Kuriyama, Y. (1989) in *Frontiers in Biotransformation* (Ruckpaul, K., & Rein, H., Eds.) Vol. 1, pp 195–243, Akademie-Verlag, Berlin.
- Gunsalus, I. C., & Sligar, S. G. (1978) *Adv. Enzymol. Relat. Areas Mol. Biol.* 47, 1–44.

- Gunsalus, I. C., Meeks, J. R., Lipscomb, J. D., Debrunner, P. G., & Münck, E. (1974) in *Molecular Mechanisms of Oxygen Activation* (Hayaishi, O., Ed.) pp 559–613, Academic Press, New York.
- Heidelberger, C. (1975) *Annu. Rev. Biochem.* **44**, 79–121.
- Hendrickson, W. A., & Konnert, J. H. (1980) in *Computing in Crystallography* (Diamond, R., Ramaseshan, S., & Venkatesan, K., Eds.) pp 1301–1323, Indian Institute of Science, Bangalore.
- Howard, A. J., Gilliland, G. L., Finzel, B. C., Poulos, T. L., Ohlendorf, D. H., & Salemme, F. R. (1987) *J. Appl. Crystallogr.* **20**, 383–387.
- Hui Bon Hoa, G., & Marden, M. C. (1982) *Eur. J. Biochem.* **124**, 311–315.
- Hui Bon Hoa, G., Di Primo, C., Dondaine, I., Sligar, S. G., Gunsalus, I. C., & Douzou, P. (1989) *Biochemistry* **28**, 651–656.
- Imai, Y., & Nakamura, M. (1989) *Biochem. Biophys. Res. Commun.* **158**, 717–722.
- Imai, Y., Shimada, H., Watanabe, Y., Matsushima-Hibiya, Y., Makino, R., Koga, H., Horiuchi, T., & Ishimura, Y. (1989) *Proc. Natl. Acad. Sci. U.S.A.* **86**, 7823–7827.
- Imai, Y., Uno, T., & Nakamura, M. (1990) in *Proceedings of the VIIIth International Symposium on Microsomes and Drug Oxidations*, p 130, Stockholm, Karolinska Institute, June 25–29, 1990.
- Jung, C., & Marlow, F. (1987) *Stud. Biophys.* **120**, 241–251.
- Lange, R., & Debey, P. (1979) *Eur. J. Biochem.* **94**, 485–489.
- Lange, R., Hui Bon Hoa, G., Debey, P., & Gunsalus, I. C. (1979) *Eur. J. Biochem.* **94**, 491–496.
- Martinis, S. A., Atkins, W. M., Stayton, P. S., & Sligar, S. G. (1989) *J. Am. Chem. Soc.* **111**, 9252–9253.
- Nebert, D. W., & Gonzalez, F. J. (1987) *Annu. Rev. Biochem.* **56**, 945–993.
- Nebert, D. W., Eisen, H. J., Negishi, M., Lang, M. A., Hjelmeland, L. M., & Okey, A. B. (1981) *Annu. Rev. Pharmacol. Toxicol.* **21**, 431–462.
- Nelson, D. R., & Strobel, H. W. (1988) *J. Biol. Chem.* **263**, 6038–6050.
- Nelson, D. R., & Strobel, H. W. (1989) *Biochemistry* **28**, 656–660.
- Ortiz de Montellano, P. R., Ed. (1986) *Cytochrome P-450. Structure, Mechanism and Biochemistry*, Plenum Press, New York.
- Peterson, J. A. (1971) *Arch. Biochem. Biophys.* **144**, 678–693.
- Poulos, T. L. (1987) *Adv. Inorg. Biochem.* **7**, 1–36.
- Poulos, T. L., & Finzel, B. C. (1984) *Pept. Protein Rev.* **4**, 115–171.
- Poulos, T. L., & Howard, A. J. (1987) *Biochemistry* **26**, 8165–8174.
- Poulos, T. L., Perez, M., & Wagner, G. C. (1982) *J. Biol. Chem.* **257**, 10427–10429.
- Poulos, T. L., Finzel, B. C., Gunsalus, I. C., Wagner, G. C., & Kraut, J. (1985) *J. Biol. Chem.* **260**, 16122–16130.
- Poulos, T. L., Finzel, B. C., & Howard, A. J. (1986) *Biochemistry* **25**, 5314–5322.
- Poulos, T. L., Finzel, B. C., & Howard, A. J. (1987) *J. Mol. Biol.* **195**, 687–700.
- Raag, R., & Poulos, T. L. (1989a) *Biochemistry* **28**, 917–922.
- Raag, R., & Poulos, T. L. (1989b) *Biochemistry* **28**, 7586–7592.
- Raag, R., & Poulos, T. L. (1991) in *Frontiers in Biotransformation* (Ruckpaul, K., Ed.) Vol. 8, Akademie-Verlag, Berlin.
- Raag, R., Swanson, B. A., Poulos, T. L., & Ortiz de Montellano, P. R. (1990) *Biochemistry* **29**, 8119–8126.
- Sato, R., & Omura, T. (1978) *Cytochrome P-450*, Academic Press, New York.
- Scheeren, J. W., Ooms, P. H. J., & Nivard, R. J. F. (1973) *Synthesis*, 149–151.
- Sligar, S. G., & Gunsalus, I. C. (1979) *Biochemistry* **11**, 2290–2295.
- Staudt, H., Lichtenberger, F., & Ullrich, V. (1974) *Eur. J. Biochem.* **46**, 99–106.
- Ullrich, V. (1979) *Top. Curr. Chem.* **83**, 67–104.
- Wagner, G. C., & Gunsalus, I. C. (1982) in *The Biological Chemistry of Iron* (Dunford, H. B., Dolphin, D., Raymond, K., & Sieker, L., Eds.) pp 405–412, Riedel, Boston.
- White, R. E., McCarthy, M.-B., Egeberg, K. D., & Sligar, S. G. (1984) *Arch. Biochem. Biophys.* **228**, 493–502.
- Wolf, C. R. (1986) *Trends Genet.* **2**, 209–214.
- Zhukov, A. A., & Archakov, A. I. (1982) *Biochem. Biophys. Res. Commun.* **109**, 813–818.